

Tailoring the magnetic properties of Fe asymmetric nanodots

B. Leighton¹, N. M. Vargas¹, D. Altbir^{1,2}, and J. Escrig^{1,2}

¹ *Departamento de Física, Universidad de Santiago de Chile,
USACH, Av. Ecuador 3493, Santiago, Chile and*

² *Center for the Development of Nanoscience and Nanotechnology,
CEDENNA, Av. Ecuador 3493, Santiago, Chile*

Asymmetric dots as a function of their geometry have been investigated using three-dimensional (3D) object oriented micromagnetic framework (OOMMF) code. The effect of shape asymmetry of the disk on coercivity and remanence is studied. Angular dependence of the remanence and coercivity is also addressed. Asymmetric dots are found to reverse their magnetization by nucleation and propagation of a vortex, when the field is applied parallel to the direction of asymmetry. However, complex reversal modes appear when the angle at which the external field is applied is varied, leading to a non monotonic behavior of the coercivity and remanence.

I. INTRODUCTION

During the last decade a great deal of attention has been focused on the study of regular arrays of magnetic particles produced by nano-imprint lithography. Besides the basic scientific interest in the magnetic properties of these systems, lithographed magnetic nanostructures are good candidates for the production of new magnetic devices, magnetic sensors and logical devices¹ as high density storage media². The properties exhibited by these nanostructures are strongly dependent on the geometry, and therefore great control of the shape is fundamental for the understanding and applications of such materials³.

In the case of nanodots, two main reversal mechanisms for the magnetization have been observed, vortex nucleation and coherent rotation⁴. Vortex states are characterized by in-plane and out-of-plane magnetization. In-plane magnetization forms the vortex chirality, a clockwise or counterclockwise magnetization rotation around a core. Out-of-plane magnetization defines the polarity, the up or down direction of the vortex core magnetization. In this way, vortices exhibit four different magnetic states and can then store the information of four magnetic bits. Switching of the vortex polarity by the application of small magnetic fields along the dot axis suggests the possibility of using the vortex for high density storage media. Methods to control chirality in single FM layer elements exploit an asymmetry in the applied field, such as using a magnetic force microscope tip^{5,6}, magnetic pulses⁷, or a magnetic field gradient⁸, as well as the magnetization history⁹. Also the geometry can be used to control polarity and/or chirality, and dots with slight geometric asymmetry^{10,11} or triangular nanodots^{6,12} have been used for this purpose.

On the other hand, some groups adopted the idea of asymmetric disks to achieve control over the vortex chirality with an in-plane magnetic field^{10–15}. Following this idea, Wu *et al.*¹¹ studied vortex nucleation, annihilation and field distribution switching in 40-nm-thick Ni₈₀Fe₂₀ disk arrays, with a diameter of 300 nm and different degrees of asymmetry. Their measurements and micromag-

netic simulations showed that the nucleation and annihilation of vortices have a linear relation with respect to the ratio of the long/short asymmetry axes, while the switching field distribution oscillates. More recently, Dumas *et al.*¹⁵ reported the synthesis and magnetic characterization of polycrystalline arrays of asymmetric Co dots where the circular shape of all the dots had been broken in the same way. In these arrays they showed how the vortices can be manipulated to annihilate at particular sites under certain field orientations and cycling sequences.

On another side, several works on magnetic nanoparticles focus on coercivity, which is strongly dependent on geometric parameters. Although current experimental facilities allow the fabrication of dots with a variety of geometries, precision is still a problem. Therefore, the possibility of controlling the coercivity by other means is highly desirable. Since coercivity is directly related to the reversal mechanism, one alternative is to induce different reversal modes by modifying external parameters, such as the direction of the applied field.

Following these ideas, in this paper, micromagnetic simulations have been used to investigate the angular dependence of the hysteresis and reversal modes for non-interacting asymmetric dots as a function of their geometry. We focus on the behavior of the coercive field and remanence and conclude that magnetic fields applied along different directions on asymmetric dots are a possible way of tailoring magnetic properties of nanodots.

II. MICROMAGNETIC BACKGROUND

The theory of micromagnetism was developed by Brown Jr. about 50 years ago¹⁶. According to this model, a ferromagnetic system consisting of a large number of individual magnetic spins is described using continuous functions for the magnetization, the fields and the energies. Moreover, the amplitude of the magnetization vector $\mathbf{M}(\mathbf{r})$ has to be constant, but its orientation may change from one position to another. In this approach, for a given magnetization distribution $\mathbf{M}(\mathbf{r})$ the

Gibbs free energy is

$$G(\mathbf{M}) = \int dV \left[A(\nabla \mathbf{m})^2 - \frac{1}{2} \mu_0 M_s (\mathbf{m} \cdot \mathbf{H}_{dem}) - \mu_0 M_s (\mathbf{m} \cdot \mathbf{H}) \right] \quad (1)$$

where \mathbf{H} is an applied field, A is the exchange constant and \mathbf{H}_{dem} is the demagnetizing field. Using the variational principle to minimize the Gibbs free energy with respect to the magnetization \mathbf{M} , the equation of the stable equilibrium state is $\mathbf{m} \times \mathbf{H}_{eff} = 0$, where the effective field \mathbf{H}_{eff} is defined as $\mathbf{H}_{eff} = -dG/d\mathbf{M}$. Because the magnetostatic interaction is of long range, analytical solutions of micromagnetic problems can only be obtained for samples of simple shape and making use of simplifying assumptions¹⁷. Because of their symmetry, ring geometries are particularly suited for such analytical calculations^{18,19}. However, for systems having a complex geometry, like asymmetric rings, numerical simulations are required.

The magnetization dynamics is governed by the Landau-Lifshitz-Gilbert equation (LLG)²⁰

$$\frac{d\mathbf{M}}{dt} = -\gamma \mathbf{M} \times \mathbf{H}_{eff} + \frac{\alpha}{M_s} \mathbf{M} \times \frac{d\mathbf{M}}{dt} \quad (2)$$

where γ is the gyromagnetic ratio of the free electron spin and α is a phenomenological damping constant. The equation describes a combined precession and relaxation motion of the magnetization in an effective field \mathbf{H}_{eff} . The calculations presented here have been computed by Oriented Micro Magnetic Framework software (OOMMF)²¹. Thus, the ferromagnetic system is spatially divided into cubic cells and within each cell the magnetization is assumed to be uniform. In order to assure a good description of the magnetization details, the size of the mesh has to be smaller than the exchange length of the material, defined by $l_{ex} = \sqrt{2A/\mu_0 M_s^2}$. The choice of the discretization scheme is validated by the fact that the numerical roughness (generated by the square mesh representation) corresponds to the real imperfections on the lateral ring surface, arising for example from the resolution of the patterning methods used.

III. SAMPLE SPECIFICATION

Our starting point is a uniform circular dot with diameter d and height h . We introduce asymmetries in these dots by cutting specific sections characterized by the parameter $\delta = r/R$, as illustrated in Fig. 1. A symmetric dot is characterized by $\delta = 1.0$, while a semicircular one is represented by $\delta = 0.0$. To simulate the magnetic properties we used micromagnetic simulations, assuming that the dot-dot distance is large enough to consider every dot as independent²². For our simulations

we use the typical Fe parameters: saturation magnetization $M_s = 1.859 \times 10^6$ A/m, exchange stiffness constant $A = 45.78 \times 10^{-12}$ J/m, and a mesh size of 2 nm, where spins are free to rotate in three dimensions. Since we are interested in polycrystalline samples, anisotropy is very small and can be safely neglected²². In all the cases the damping parameter was chosen as 0.5.

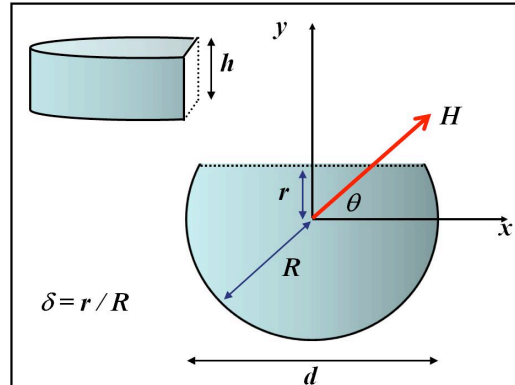


FIG. 1. (Color online) Geometrical parameters of a nanodot. The white surface represents the section that has been cut.

IV. RESULTS AND DISCUSSION

A. Magnetic field applied parallel to the x axis

Our main concern in this work is to investigate the role of the asymmetric shape of the disk in the coercivity and reversal mechanisms of the magnetization. The hysteresis curves for different diameters and δ , with $h = 20$ nm, are illustrated in Fig. 2, where we see for all diameters an almost square loop with coercivities strongly dependent on the geometry. For all diameters and $\delta = 1.0$ the dots exhibit a small coercivity, which increases while decreasing δ .

In Figs. 3 and 4 we illustrate the general behavior of a dot for different values of h and δ . In these figures we observe a non-monotonic behavior of coercivity and remanence which is the result of a competition between exchange, local dipolar interactions and geometry in the region where the cut is made. Once we have a small asymmetry ($\delta = 0.9$) in some cases a decrease of the coercivity and remanence is seen. However, for further decreases of δ , remanence and coercivity are almost constant or grow continuously.

In order to understand this behavior we look at snapshots of the hysteresis and observe that the magnetization reversal occurs by a C formation followed by vortex nucleation and propagation. This behavior is illustrated in Fig. 5(a) for $d = 60$ nm, $h = 20$ nm and each of the three values of δ used in Fig. 2. Looking at these snapshots we can conclude that a vortex nucleates during the

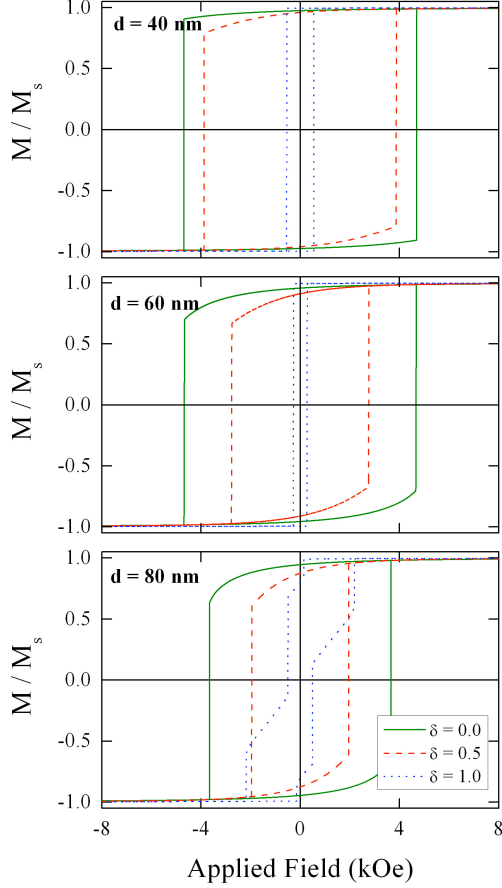


FIG. 2. (Color online) Hysteresis loops for asymmetric dots with height $h = 20$ nm for different diameters and δ values.

reversal for any value of δ . In symmetric dots, square loops are a sign of coherent reversal, and the appearance of a neck indicates that the reversal is driven by a vortex nucleation and propagation²². However for asymmetric dots reversal by vortex nucleation may lead to a square loop.

Once a cut is made on the dot, a magnetic pole is formed on the new surface. Due to the Pole Avoidance Principle¹⁷, a C state nucleates in order to avoid the formation of a magnetic pole, followed by the nucleation of a vortex. However, when the asymmetry increases by cutting larger sections of the dot, the local effects described above compete with the new geometry, that is, the lack of circular symmetry, making vortex formation more difficult. Then, in this last case, C formation and vortex nucleation become more difficult compared with the situation when a small cut is made or a symmetric dot is considered, and an increase in coercivity and remanence appears.

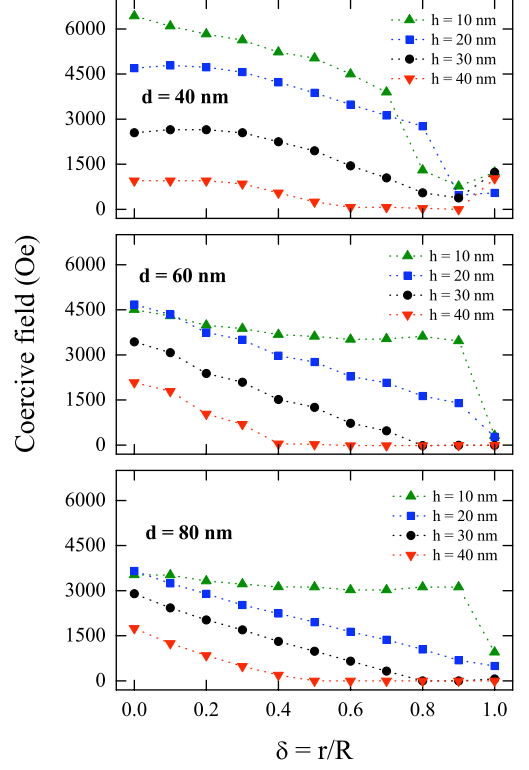


FIG. 3. (Color online) Coercivity of asymmetric dots for different height h , diameter d and δ values.

B. Angular dependence of the coercivity

We also investigated the angular dependence of the magnetization, applying a magnetic field along a direction defined by θ , which is the angle between the applied field direction and the x axis, as illustrated in Figure 1. Our results for $d = 60$ nm and $h = 20$ nm are depicted in Figs. 6 and 7. While symmetric dots show no angular dependence, as expected, asymmetric dots exhibit a strong angular dependence. By increasing θ the coercivity decreases drastically until zero and a non hysteretic behavior is observed for $\theta = 90^\circ$. This behavior allows us to conclude that shape anisotropy of an asymmetric dot may induce a hard axis of magnetization when $\theta = 90^\circ$.

Besides, the magnetization inside an asymmetric dot is oriented parallel to the x axis (easy axis), due to the shape anisotropy. When the applied field is reduced to zero, at remanence, each dot presents its magnetization along the axis, but it is measured at an angle θ with respect to the easy axis. Then, one can approximate the remanence of an asymmetric dot by $M_R(\theta) = M_R \cos^2(\theta)$, with $M_R = M_R(\theta = 0)$ the remanence measured at $\theta = 0$. This behavior is an indication that asymmetric dots follow the behavior of uniaxial systems. Finally it is important to note that results for the remanence for $\delta = 0.0$ and 0.5 almost coincide.

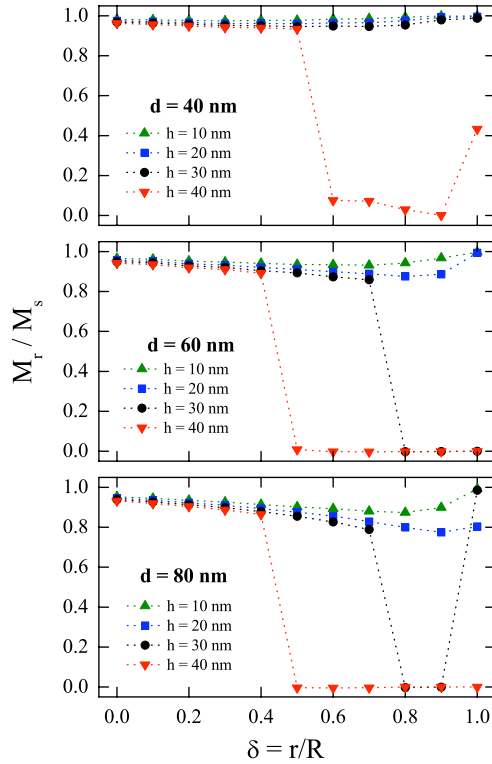


FIG. 4. (Color online) Remanence of asymmetric magnetic dots as a function of δ .

To understand this behavior, snapshots of the reversal of the magnetization are depicted in Fig. 5(b) and 5(c). It is seen that for $\delta = 0.5$ the reversal occurs by means of the nucleation and propagation of a vortex. For $0^\circ \leq \theta < 30^\circ$, the vortex nucleates at the center of the horizontal surface, and propagates along the y direction until it is annihilated at the opposite end of the dot. For $30^\circ \leq \theta \leq 60^\circ$, the vortex nucleates at the center of the horizontal surface and propagates along the x direction until it is annihilated at one end of the horizontal surface. For $60^\circ < \theta \leq 90^\circ$, a coherent reversal occurs.

For $\delta = 0.0$ the reversal of the magnetization occurs through the nucleation of a C state and further nucleation and propagation of a vortex. For $0^\circ \leq \theta \leq 60^\circ$, two regions of different magnetic orientation appear. These regions start growing until the full inversion of the magnetization occurs. For $60^\circ < \theta \leq 90^\circ$, a coherent reversal occurs. The non monotonic behavior of the coercivity in Fig. 7 can be explained by the existence of different reversal modes as a function of θ .

V. CONCLUSIONS

The results presented above show that the existence of asymmetry strongly modifies the magnetic behavior of a

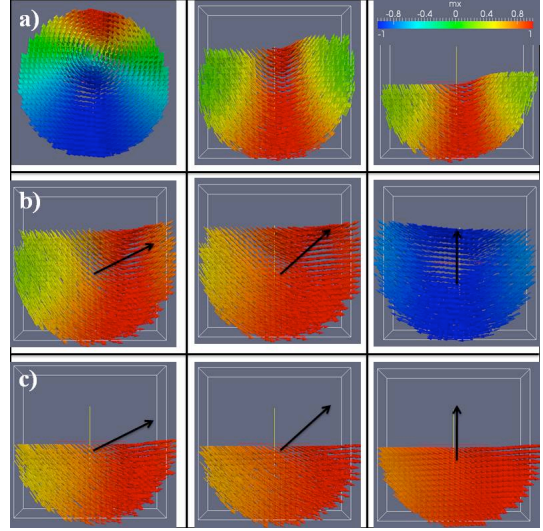


FIG. 5. Snapshots of the magnetization of the dot during the reversal for a) $\delta=1.0$, $\delta = 0.5$ and $\delta = 0.0$ when $\theta= 0$, b) $\theta=30$, 60 and 90 when $\delta = 0.5$, and c) $\theta=30$, 60 and 90 when $\delta = 0.0$. The arrows illustrate the direction of the magnetic moments.

dot. In this case the coercivity and remanence are drastically modified as a function of δ when a magnetic field is applied parallel to the x axis. Also we have extended our results to the case of an angular dependence of the coercivity and remanence, where a transition from vortex-mode to coherent-mode rotation has been observed. In this way asymmetry can be useful for tailoring specific magnetic characteristics of these systems. However, experimental work remains to be done in order to observe this transition.

ACKNOWLEDGMENTS

Support from FONDECYT under projects 11070010 and 1080300; the Millennium Science Nucleus “Basic and Applied Magnetism” P06-022-F; and Financiamiento Basal para Centros Científicos y Tecnológicos de Excelencia under project FB0807 is gratefully acknowledged.

¹ R. P. Cowburn, M. E. Welland, Science **287** (2000) 1466.

² J. N. Chapman, P. R. Aitchison, K. J. Kirk, S. McVitie, J. C. S. Kools, M. F. Gillies, J. Appl. Phys. **83** (1998) 5321.

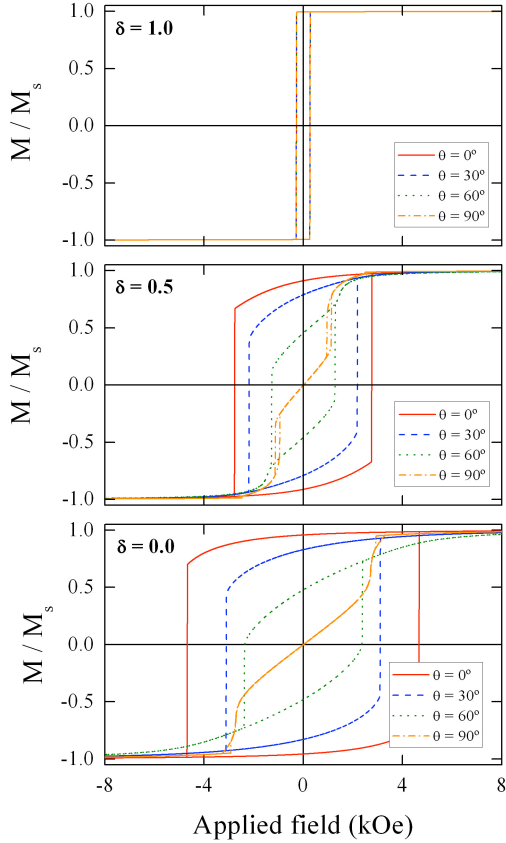


FIG. 6. (Color online) Hysteresis loops for asymmetric dots with diameter $d = 60$ nm and height $h = 20$ nm for different angles and δ values.

- ⁹ M. Klaui, J. Rothman, L. Lopez-Diaz, C. A. F. Vaz, J. A. C. Bland, Z. Cui, Appl. Phys. Lett. **78** (2001) 3268.
- ¹⁰ M. Schneider, H. Hoffmann, J. Zweck, Appl. Phys. Lett. **79** (2001) 3113.
- ¹¹ K. M. Wu, L. Horng, J. F. Wang, J. C. Wu, Y. H. Wu, C. M. Lee, Appl. Phys. Lett. **92** (2008) 262507.

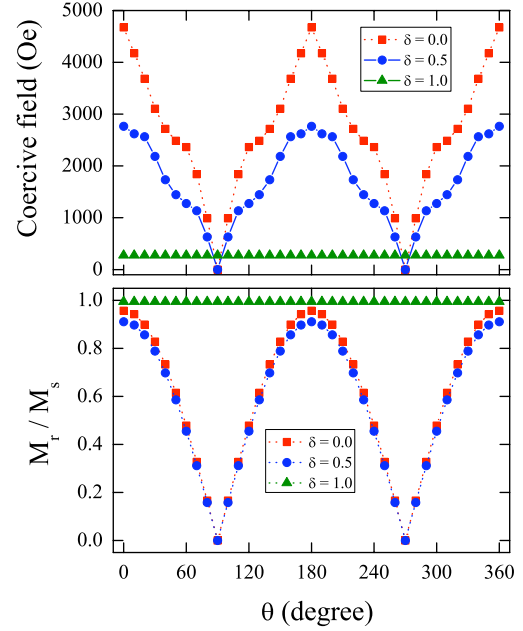


FIG. 7. (Color online) Coercivity and remanence of asymmetric dots with diameter $d = 60$ nm and height $h = 20$ nm for different angles and δ values.

- ³ C. Ross, Annu. Rev. Mater. Res. **31** (2001) 203.
- ⁴ I. V. Roshchin, C. -P. Li, H. Suhl, X. Battle, S. Roy, S. K. Sinha, S. Park, R. Pynn, M. R. Fitzsimmons, J. Mejía-López, D. Altbir, A. H. Romero, I. K. Schuller, Europhys. Lett. **86** (2009) 67008.
- ⁵ V. L. Mironov, B. A. Gribkov, A. A. Fraerman, S. A. Gusev, S. N. Vdovichev, I. R. Karetnikova, I. M. Nefedov, I. A. Shere-shevsky, J. Magn. Magn. Mater. **312** (2007) 153.
- ⁶ M. Jaafar, R. Yanes, D. Perez de Lara, O. Chubykalo-Fesenko, A. Asenjo, E. M. Gonzalez, J. V. Anguita, M. Vázquez, J. L. Vicent, Phys. Rev. B **81** (2010) 054439.
- ⁷ Y. Gaididei, D. D. Sheka, F. G. Mertens, Appl. Phys. Lett. **92** (2008) 012503.
- ⁸ M. Konoto, T. Yamada, K. Koike, H. Akoh, T. Arima, Y. Tokura, J. Appl. Phys. **103** (2008) 023904.
- ¹² P. Vavassori, R. Bovolenta, V. Metlushko, B. Ilic, J. Appl. Phys. **99** (2006) 053902.
- ¹³ T. Taniuchi, M. Oshima, H. Akinaga, K. Ono, J. Appl. Phys. **97** (2005) 10J904.
- ¹⁴ F. Giesen, J. Podbielski, B. Botters, D. Grundler, Phys. Rev. B **75** (2007) 184428.
- ¹⁵ R. K. Dumas, T. Gredig, C. P. Li, I. K. Schuller, K. Lai, Phys. Rev. B **80** (2009) 014416.
- ¹⁶ W. F. Brown Jr., Micromagnetics, Wiley, New York, 1963.
- ¹⁷ A. Aharoni, Introduction to the Theory of Ferromagnetism, Clarendon, Oxford, 1996.
- ¹⁸ M. Beleggia, J. W. Lau, M. A. Schofield, Y. Zhu, S. Tandon, M. De Graef, J. Magn. Magn. Mater. **301** (2006) 131.
- ¹⁹ P. Landeros, J. Escrig, D. Altbir, M. Bahiana, J. d'Albuquerque e Castro, J. Appl. Phys. **100** (2006) 044311.
- ²⁰ T. L. Gilbert, Phys. Rev. **100** (1955) 1243.
- ²¹ M. J. Donahue, D. G. Porter, OOMMF User's Guide, Version 1.2a3, 2002. <http://math.nist.gov/oommf>.
- ²² J. Mejía-Lopez, D. Altbir, P. Landeros, J. Escrig, A. H. Romero, Igor V. Roschin, C. -P. Li, M. R. Fitzsimmons, X. Battle, Ivan K. Schuller, Phys. Rev. B **81** (2010) 184417.